OPEN

ARTICLE

Citation: Cell Discovery (2015) 1, 15004; doi:10.1038/celldisc.2015.4

www.nature.com/celldisc

High-yield production of extracellular type-I cellulose by the cyanobacterium *Synechococcus* sp. PCC 7002

Chi Zhao[1,2,*], Zhongkui Li[2,*], Tao Li[3,*], Yingjiao Zhang[1], Donald A Bryant[2,4], Jindong Zhao[1,3]

[1]*State Key Laboratory of Protein and Plant Genetic Engineering, College of Life Sciences, Peking University, Beijing, China;* [2]*Department of Biochemistry and Molecular Biology, The Pennsylvania State University, University Park, PA, USA;* [3]*CAS Key Laboratory of Phycology, Institute of Hydrobiology, Chinese Academy of Sciences, Wuhan, Hubei, China;* [4]*Department of Chemistry and Biochemistry, Montana State University, Bozeman, MT, USA*

Cellulose synthase, encoded by the *cesA* gene, is responsible for the synthesis of cellulose in nature. We show that the cell wall of the cyanobacterium *Synechococcus* sp. PCC 7002 naturally contains cellulose. Cellulose occurs as a possibly laminated layer between the inner and outer membrane, as well as being an important component of the extracellular glycocalyx in this cyanobacterium. Overexpression of six genes, *cmc–ccp–cesAB–cesC–cesD–bgl,* from *Gluconacetobacter xylinus* in *Synechococcus* sp. PCC 7002 resulted in very high-yield production of extracellular type-I cellulose. High-level cellulose production only occurred when the native *cesA* gene was inactivated and when cells were grown at low salinity. This system provides a method for the production of lignin-free cellulose from sunlight and CO_2 for biofuel production and other biotechnological applications.

***Keywords*:** synthetic biology; photosynthesis; cellulose; cell wall; bioethanol

Cell Discovery (2015) **1,** 15004; doi:10.1038/celldisc.2015.4; published online 28 April 2015

Introduction

Cellulose is the most abundant biopolymer in nature. It accounts for about half of the CO_2 fixed through photosynthesis and is critically important to our society because of its uses in the wood, paper, and fiber industries. Cellulose utilization as a biofuel is increasing rapidly [1–4], and it also has important uses in biomedical applications [5]. Cellulose is a long-chain polymer of D-glucose molecules joined by β-1,4-glycosidic bonds, and it is an important structural component of the cell walls of higher plants, algae, fungi, and some bacteria [6]. Cellulose forms crystalline microfibrils that group to form bundles, which in turn form 'ribbons'. A pellicle of cellulose is formed from a random assemblage of fibrils (< 130 nm wide), which are composed of a bundle of much finer microfibrils (2–4 nm in diameter). Bacterial cellulose is distinguished from plant cellulose by having a high crystallinity index (> 60%). There are two common forms of crystalline cellulose, denoted type I and II, which can be distinguished by X-ray diffraction and other spectroscopic methods. Type-I cellulose is formed from laterally and unidirectionally aligned, parallel β-1,4-glucan chains; the glucan chains in type-II cellulose are arranged in an antiparallel manner [6].

Cellulose is synthesized by cellulose synthases [7–10], which form terminal complexes and are composed of at least five polypeptides (BcsABCD and Ccp) in the bacterium *Gluconacetobacter xylinus* [11, 12]. The genes encoding cellulose synthases, variously denoted as *ces*, *acs*, or *bcs,* and related proteins are often organized in operons (for example, *cmc–ccp–cesAB–cesC–cesD–bgl* for *G. xylinus*) [13–15]. Terminal complexes span the inner and outer membranes and are usually organized in rows along the longitudinal axis of the cell [16, 17]. In *Rhodobacter sphaeroides* a BcsA–BcsB heterodimer catalyzes and regulates cellulose synthesis, and the structure of this complex was recently determined at 3.25-Å resolution

*These three authors contributed equally to this work.
Correspondence: Donald A Bryant
Tel: +1-814-865-1992; Fax: +1-814-863-7024;
E-mail: dab14@psu.edu
or Jindong Zhao
Tel: +86-10-62756421; Fax: +86-10-62754427;
E-mail: jzhao@pku.edu.cn
Received 5 January 2015; accepted 7 January 2015

together with a translocating glycan chain [18]. The glycosyltransferase domain and active site occurs in the cytoplasm, and the membrane-intrinsic portion forms a cellulose-conducting channel. BcsA contributes eight transmembrane α-helices to this channel, whereas the periplasmic protein BcsB contributes one transmembrane α-helix that anchors this protein to the membrane. The structure suggests a model in which cellulose is synthesized at the cytoplasmically localized active site and translocated through the cytoplasmic membrane one glucose residue at a time [18]. The cellulose-synthesizing activity of BcsA is strongly stimulated by cyclic-di-GMP, which binds to a PilZ domain that occurs at the C terminus of BcsA and which lies close to the glycosyltransferase active site [18].

In *G. xylinus*, CesC and CesD are involved in cellulose secretion and crystallization, which may be the rate-limiting steps of cellulose synthesis [11–15, 18, 19]. Additional proteins, including periplasmic endoglucanases, also have roles in cellulose synthesis and secretion [9, 12, 14, 20, 21]. Higher plant genomes encode multiple copies of *cesA*, but no homologs of the other bacterial *ces* genes and related proteins have been identified [10, 22]. Several cyanobacteria, which are oxygenic photoautotrophs like plants, have *cesA* genes encoding proteins with sequence similarity to bacterial and plant cellulose synthases, but similar to plants, no other *ces*/*bcs* genes have been identified to date in cyanobacterial genomes [23]. Cellulose microfibers, which may have a role in cellular aggregation, have been reported in cyanobacteria [23, 24]. However, little biochemical and genetic evidence directly connects cyanobacterial CesA with cellulose synthesis.

To characterize CesA function in the euryhaline cyanobacterium *Synechococcus* sp. PCC 7002 (hereafter *Synechococcus* 7002) and to explore the potential of cyanobacteria for cellulose production for biotechnological applications, we constructed and characterized a *cesA* (SynPCC7002_A2118) null mutant. We report here that cellulose is an important component of the cell wall and glycocalyx of *Synechococcus* 7002. We additionally show that high-level production of type-I cellulose can be achieved in *Synechococcus* 7002 by heterologous overexpression of a six-gene cassette from *G. xylinus* under appropriate environmental conditions.

Results

Cellulose layer in the cell wall of Synechococcus 7002

The genome of *Synechococcus* 7002 encodes an open-reading frame, SynPCC7002_A2118, that predicts a protein with strong sequence similarity to previously characterized *cesA* gene products, which have been shown to be cellulose synthases. SynPCC7002_A2118 predicts a protein of 788 amino acids, which is slightly larger than the characterized cellulose synthase of *Nostoc* sp. PCC 7120 (693 amino acids; 54% identical, 70% similar) [23] because of an insertion of ~90 amino acids. However, this CesA is identical in size to the BcsA protein of *R. sphaeroides*, whose X-ray structure is known [18] and is ~30% identical and ~45% similar in sequence. Similar proteins were found in about 20 other cyanobacterial genomes, as well as in the genomes of numerous bacteria known to synthesize bacterial cellulose. Many of the cyanobacteria are soil, benthic, or colonial organisms, in which cellulose might have a structural role in mat or colony formation. Interestingly, the mat-forming organisms *Chloroflexus* spp. and *Roseiflexus* spp. (phylum *Chloroflexi*), as well as the purple non-sulfur bacterium, *R. sphaeroides* (phylum *Proteobacteria*), are other commonly studied chlorophototrophic bacteria that have *cesA*/*celA*/*bcsA* genes and thus presumably have the ability to synthesize cellulose. However, most purple bacteria do not have a gene for cellulose synthase and thus cannot synthesize cellulose.

To study the function of CesA in *Synechococcus* 7002, we constructed a *cesA* null mutant and compared its properties with those of the wild type (WT) under different growth conditions. The WT grew equally well (doubling time $= 4.5 \pm 0.2$ h) at low salinity (that is, in medium BG-11) or in a high salinity, artificial seawater medium (medium A^+) [25]. The doubling time for the *cesA* mutant was the same as the WT in medium A^+; however, the *cesA* mutant grew much more slowly (doubling time $= 9.8 \pm 0.4$ h) than the WT at low salinity. Scanning electron microscopy showed that the *cesA* mutant formed numerous elongated cells and minicells when grown at low salinity (Figure 1d), which accounted for 5% (±0.4%) and 23% (±1.4%) of total cell numbers, respectively. These cells were not observed for WT (Figures 1a and b) or when the *cesA* mutant was grown at higher salinity (Figure 1c).

Cyanobacteria have a Gram-negative cell wall, and previous studies had suggested that their peptidoglycan (PG) layer is thicker than that of most other Gram-negative bacteria [26]. We used transmission electron microscopy to study the cell walls of *Synechococcus* 7002 strains. A cell wall layer between the cytoplasmic and outer membranes was clearly observed in thin sections of the WT (Figure 2a), but this layer was

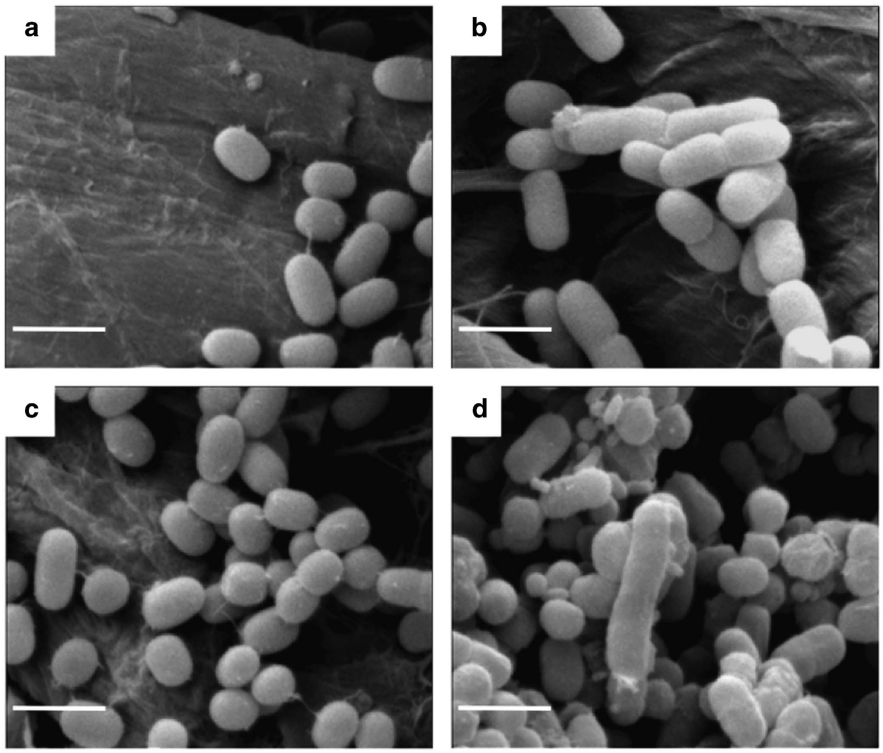

Figure 1 Scanning electron microscopy (SEM) study of cell morphology of wild type (**a**, **b**) and c*esA* mutant (**c**, **d**) strains of *Synechococcus* 7002 grown in A^+ medium (**a**, **c**) or BG-11 medium (**b**, **d**). Scale bar, 2 μm.

absent in the *cesA* mutant (Figure 2b). This layer also disappeared when WT cells were incubated with cellulase in the presence of 2 mM EDTA (Figure 2c), which suggested that this wall contained cellulose whose synthesis was dependent on the presence of functional CesA. This suggestion is further supported by the finding that the periplasm and cell surface could specifically be labeled with a cellulose-binding domain protein detected by immunogold labeling (Figure 3). No labeling was observed when *cesA* mutant cells were subjected to the same treatment (data not shown). When ultrathin sections of WT cells were stained with ruthenium red [27], this layer was visible as a distinct layer (Figure 2d), which we interpret to be laminated, but this layer was not observed in cell walls of a *cesA* mutant (Figure 2e). A careful analysis of these images suggested that this layer was located between the PG layer (Figure 2d, white arrows) and the outer membrane. Ruthenium red staining also revealed polysaccharides on the outer surface of the outer membrane in WT cells (Figure 2d) that were visibly much less abundant in the *cesA* mutant (Figure 2e). The distinctive cellulose layer in the cell wall was fully restored when the *cesA* mutant was complemented *in trans* with *cesA* (Figures 4a and c). When the *yfp* gene, encoding the yellow fluorescent protein, was fused to the *cesA* gene and transformed into a *cesA* mutant of *Synechococcus* 7002, the fusion gene also restored the cell wall structure to WT, although the cells obviously had much more surface-associated cellulose (note the intense ruthenium red staining in the periplasm as well as the extracellular glycocalyx in Figure 4c). The CesA–YFP fusion protein was localized on the cytoplasmic membranes by confocal microscopy (Figure 2f). Little or no fluorescence from YFP was observed in the cytoplasm in these confocal images, although fluorescence from chlorophyll *a* in the cytoplasm was readily apparent in the central regions of cells (data not shown). Consistent with our interpretation of the localization of YFP, the fluorescence from chlorophyll *a* did not overlap with that of YFP in merged images (data not shown). The uniform, nonpunctate distribution of CesA–YFP on the cytoplasmic membrane, together with the fact that no other *ces* genes have been identified in this cyanobacterium, suggest that CesA may not be organized into terminal complexes in *Synechococcus* 7002.

Although it was difficult to observe the PG layer directly in *cesA* mutant cells by transmission electron microscopy (however, see white arrows in Figures 2d

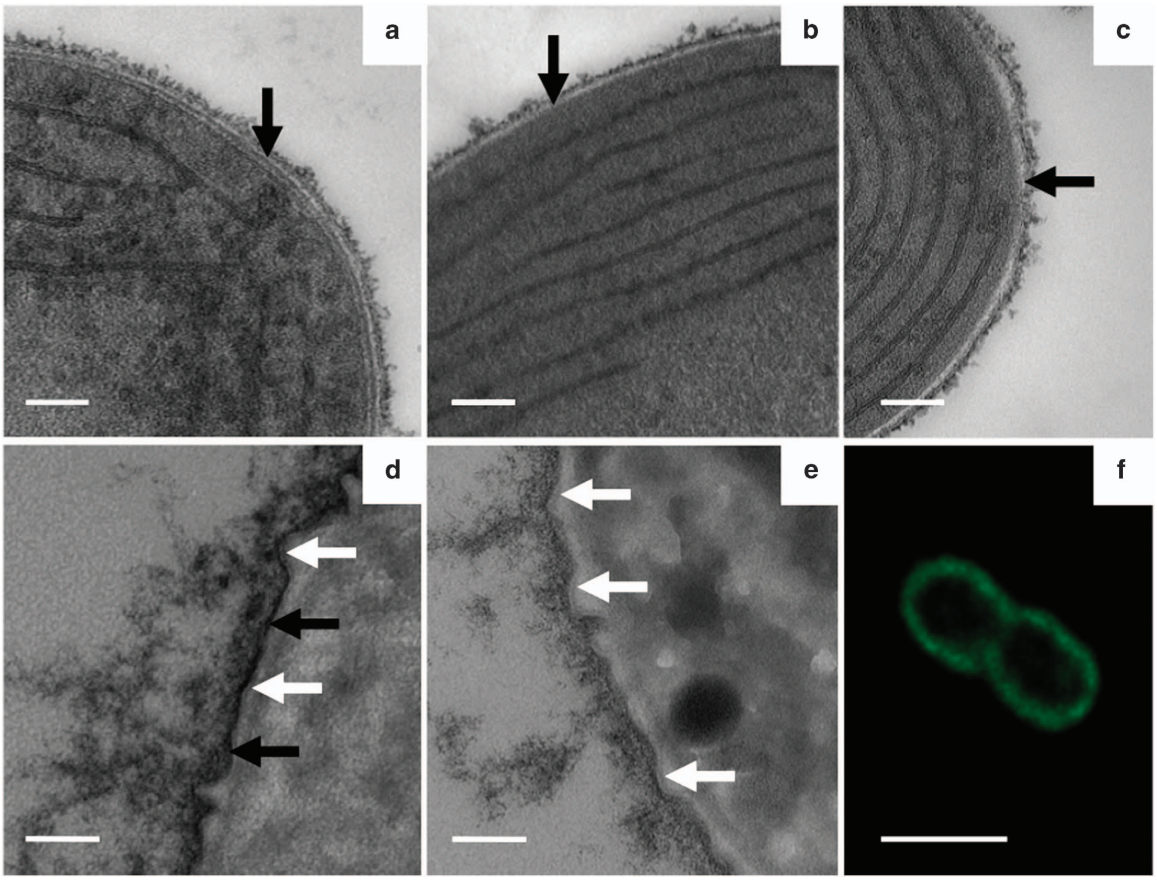

Figure 2 Transmission electron microscopy (TEM) study of cell walls in thin sections of *Synechococcus* 7002. (**a**) Wild type (WT). (**b**) *cesA* mutant. (**c**) WT cells incubated in a cellulase solution (200 μg/ml in the presence of 2 mM EDTA) for 30 min at 37 °C. The arrow in **a** indicates the electron-dense layer, and the arrows in **b** and **c** indicate its absence. Note that there is more cell-surface-associated glycocalyx material in **a** than in **b** or **c**. (**d**, **e**) TEM images of thin sections of *Synechococcus* 7002 cells stained with ruthenium red showing the changes in the cell wall and glycocalyx of WT (**d**) and a *cesA* deletion mutant (**e**), respectively. The black arrows indicate the possibly laminated, CesA-dependent cellulose layer, and the white arrows indicate the thin peptidoglycan layer. Although it was easier to see on lower-magnification images (data not shown), these images show less ruthenium red staining for the *cesA* mutant (**e**), more staining for the WT (**d**), and much more staining for a strain overproducing CesA (see Figure 4c). These data show that the *cesA* mutant had the least surface-associated polysaccharides and that the strain overproducing CesA had the most. An electron-opaque, laminated layer near the outer membrane in WT (black arrows in **d**) was missing in the *cesA* mutant (**e**). This layer apparently corresponds to the cellulose layer observed between the peptidoglycan (white arrows in **d** and **e**) and outer membrane layers in thin sections in **a**. (**f**) Confocal fluorescence microscopy showing spectrally deconvoluted, Z-stack image of *Synechococcus* 7002 cells expressing CesA–YFP. This image shows the absence of YFP fluorescence in the cytoplasm and thylakoid membranes, which could easily be visualized by fluorescence from chlorophyll *a* (data not shown). Scale bars, 100 nm (**a-e**) and 2 μm (**f**).

and e), the following evidence suggests that a PG layer was still present. The *cesA* mutant cells were viable, could still grow and divide, and were still sensitive to lysozyme treatment; moreover, a lysozyme-sensitive PG fraction could be isolated from the mutant cells (Figure 4d). Mass spectrometry showed that *N*-acetylglucosamine was present in the hydrolyzate from this fraction (Supplementary Figure S1). These results suggested that the cell wall layer between the outer membrane and plasma membrane in *Synechococcus* 7002 is composed of a thin inner PG layer and a thicker, possibly laminated, outer cellulose layer. A major component of this outer layer is cellulose produced by CesA (Figure 5). Cellulose, which was more abundant in a strain overproducing CesA (Figure 4c), was also apparently associated with the glycocalyx outside the outer membrane. Because at least 20 cyanobacterial genomes encode homologs of *cesA,* cellulose is probably a component of many but not all cyanobacterial cell walls.

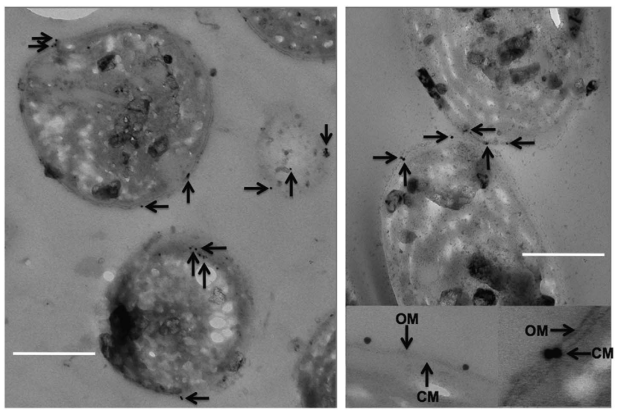

Figure 3 Immunolocalization of cellulose in *cesA* mutant complemented with *cesA–yfp* expressed from the P_{cpcAB} promoter of *Synechocystis* sp. PCC 6803 (see Materials and Methods for details). The recombinant fusion protein rCBDs-Protein L (Sigma) was used to bind to cellulose selectively, and the cellulose-binding protein was detected using goat anti-mouse IgG conjugated to 10-nm colloidal gold particles (Sigma, St Louis, MO, USA) as the second antibody. Gold particles (arrows) were predominantly observed directly over the periplasmic space and at the peripheral surface of the outer membrane (OM) of the cell wall (associated with the glycocalyx). The insets at the lower right portion of the right panel show enlargements of gold particles associated with the periplasmic space and the glycocalyx just beyond the OM. The arrows in the inset show the OM and the cytoplasmic membrane (CM). Scale bar, 500 nm.

High-yield production of cellulose in Synechococcus 7002

In an attempt to overproduce extracellular cellulose in photoautotrophic *Synechococcus* 7002, we first tried to express the native *cesA* gene under a strong P_{cpcBA} promoter from *Synechocystis* sp. PCC 6803. Although cells appeared to produce more surface-associated polysaccharides than WT (compare Figure 4c with Figures 2d and e), cellulose production did not increase markedly. Likewise, no significant extracellular cellulose production was observed when the *cesAB–cesC–cesD* operon from *G. xylinus* ATCC 53582 was inserted into the chromosome or the high-copy plasmid pAQ1 [28] in either the WT or *cesA* mutant strains of *Synechococcus* 7002. We next constructed a bacterial artificial chromosome (BAC) library of genomic DNA from *G. xylinus* using a BAC vector that can stably integrate foreign DNA into the *Synechococcus* 7002 chromosome. We transformed both the WT and *cesA* mutant with the BAC clones and screened for high-level production of cellulose among the transformants by staining with Calcofluor white, a dye that detects polymers with β-1,4-glycosidic bonds [29]. A positive strain (strain 56) was identified among transformants derived from the *cesA* mutant, and transmission electron microscopy revealed that the cellulose layer had been restored in the cell walls (Figure 4b). The corresponding BAC clone (clone 38) was isolated and sequenced, and the cloned fragment included the *cesAB–cesC–cesD* operon together with its flanking regions.

To improve the cellulose yield, various combinations of the *ces* operon and its flanking genes were inserted onto plasmid pAQ1 [28]. Transformants were tested under different growth conditions, and only one strain (CM12) in the *cesA* mutant background exhibited greatly enhanced cellulose production. Strain CM12 contained two upstream genes (*cmc* and *ccp* (cellulose complementing protein)) and one downstream gene (*bgl*) that flank the *cesAB–cesC–cesD* operon; this DNA fragment was named the cellulose synthesis module (CSM) (Supplementary Figure S2). Cellulose production by strain CM12 was strongly stimulated by transferring the cells from medium A^+ to medium BG-11. Under the latter conditions, the total cellulose content reached ~14% of the cell dry weight within 12 days (Figure 6a). Fluorescence microscopy revealed that cells accumulating cellulose exhibited strong blue fluorescence when excited with ultraviolet light in the presence of Calcofluor white. The typical red fluorescence from the photosynthetic pigments was nearly completely obscured (Figure 6b), and the color of the culture gradually changed from blue-green to white (Figure 6c). The white cultures contained cell aggregates (Figure 6d), and the cells of such cultures eventually bleached and died (Supplementary Figures S3 and S4).

The reason(s) for cell death is not clear, but it might be related to severe depletion of intracellular carbon reserves because of excessive cellulose synthesis. Alternatively, it might be due to light limitation imposed when cells were encapsulated in cellulose fibers. Because the cells bleach, it is also possible that hyperproduction of cellulose may trigger the formation of reactive oxygen species or damage the cell membranes. Surprisingly, WT cells transformed with the CSM produced very little cellulose even when grown in hyposaline medium. Thus, maximal cellulose production from the heterologous expression of the CSM genes by *Synechococcus* 7002 required that two conditions were satisfied: (i) the endogenous, native *cesA* gene had to be inactivated, and (ii) cells had to be grown under hyposaline conditions. Hyposaline growth conditions might allow cells to divert metabolic resources that would otherwise be used for the production of compatible solutes toward cellulose

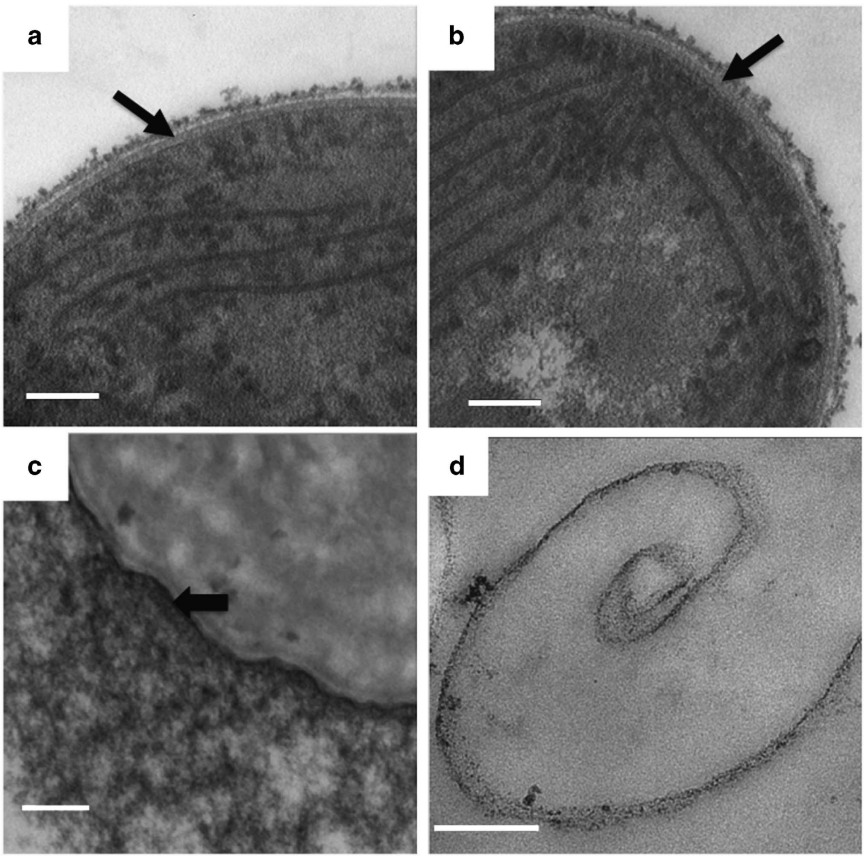

Figure 4 Transmission electron microscopy (TEM) analysis of thin sections of a *cesA* insertion mutant that was complemented with a wild-type *cesA* gene (**a**) and bacterial artificial chromosome clone 38 (**b**) (see main text for details), respectively. The black arrows indicate the cellulose layer that has been restored in both cases. (**c**) Thin-section electron micrograph after ruthernium red staining of the *cesA* deletion mutant of *Synechococcus* 7002 complemented with *cesA::yfp* under the control of the P_{cpcBA} promoter of *Synechocystis* sp. PCC 6803. The black arrow indicates the possibly laminated cellulose layer has been restored by complementation with the *cesA::yfp* fusion gene. Note the increased amount of ruthenium-red-stainable polysaccharide on the external surface of the cell compared with wild type or the *cesA* mutant (compare with Figures 2d and e). (**d**) TEM image of isolated peptidoglycan from the *cesA* mutant. Scale bar, 100 nm.

Figure 5 Schematic of cell wall structure of the cyanobacterium *Synechococcus* 7002. CL, possibly laminated layer with cellulose as a major component; CM, cytoplasmic membrane; GC, glycocalyx layer; OM, outer membrane; PG, peptidoglycan.

synthesis [30, 31]. An intriguing possibility is that hyposaline conditions might cause intracellular levels of cyclic-di-GMP levels to increase, which could stimulate CesAB activity by binding to its PilZ domain [32].

When cells of strain CM12 were examined by scanning electron microscopy, a very large amount of microfibrillar (μm size range) material was observed, which was absent after cells had been treated with cellulase (Figure 7a). This observation strongly implied that this fibrous material was cellulose. Normal cellular morphology was not fully restored in strain CM12, which still formed minicells. The fibrous extracellular material was isolated and analyzed by X-ray diffraction. Its X-ray diffraction pattern (Figure 7b) was very similar to the pattern obtained for type-I cellulose produced by *G. xylinus* [33, 34]. Although peaks 101, 10$\bar{1}$, and 040 were broadened, the peak at 23° corresponded well with diffraction peak 002 of type-I cellulose. This peak, and the overall similarities of the diffraction patterns, led us to conclude that, even though some impurities were present in the sample as

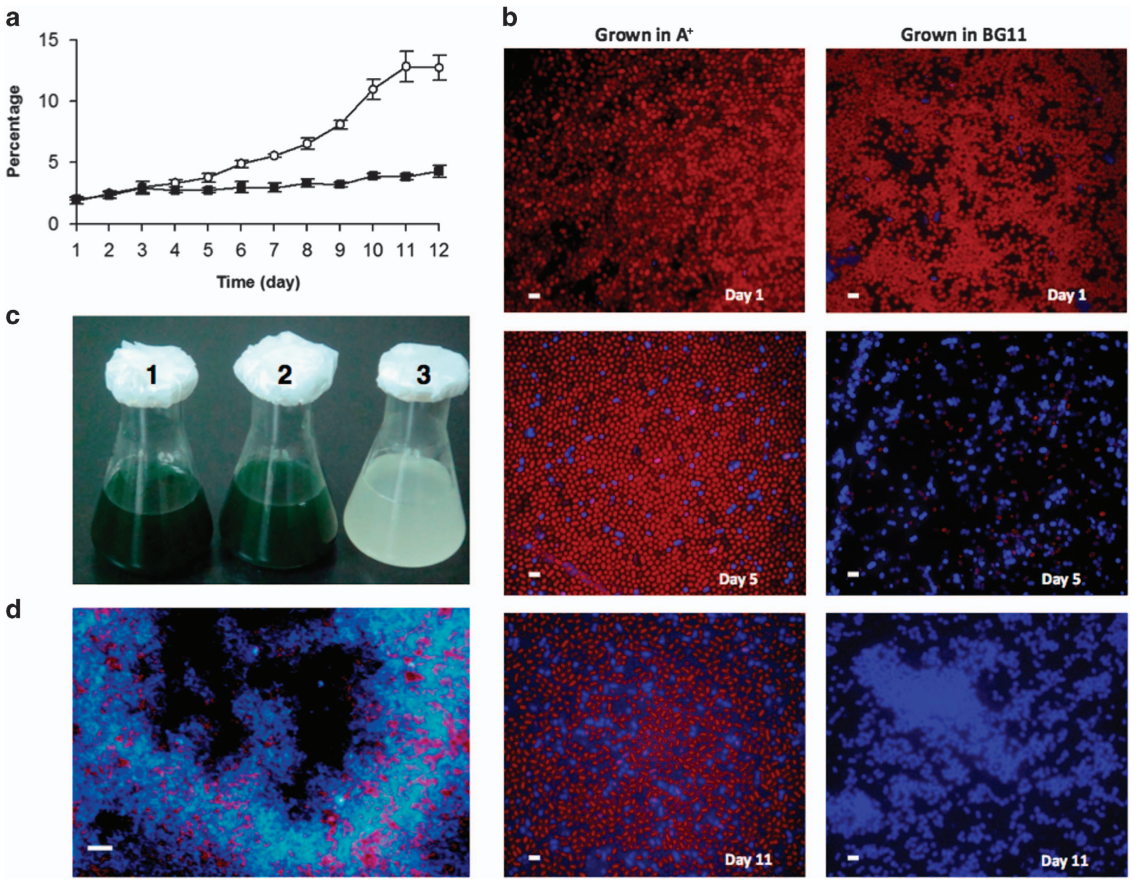

Figure 6 Cellulose production by strain CM12 after introduction of the CSM genes into the *cesA* mutant strain of *Synechococcus* 7002. (**a**) Time course of cellulose production at high salinity (medium A^+, filled circles) or low salinity (medium BG-11, open circles). Each point is the average of three measurements, and the bars show the s.e. Cellulose content was measured as glucose content and expressed as percentage of the dry weight of isolated cells (indicated as 'percentage' on the *y* axis of the figure). (**b**) Fluorescence microscopy of the Calcofluor-stained cells of strain CM12 grown at high salinity (medium A^+, left panels) or low salinity (medium BG-11, right panels) for the times indicated. Fluorescence was excited with ultraviolet (UV) light. The red fluorescence emission emanates from photosynthetic pigments and the bright blue fluorescence emission comes from Calcofluor cellulose. Scale bar, 5 μm. (**c**) Batch cultures of the wild type (1) and strain CM12 at high salinity (medium A^+) (2) or after transfer from high to BG-11 medium (low salinity) (3) for 2 weeks. The cultures (1) and (2) were both in stationary phase and their optical densities at 750 mm were ~2. (**d**) Fluorescence of the cells in flask (3) of **c**. Fluorescence in the absence of Calcofluor white was also excited with UV light. Scale bar, 20 μm. CSM, cellulose synthesis module.

indicated by the peaks at 27° and 28.5°, the isolated material contained type-I cellulose. The crystallinity index of the celluloses produced by *G. xylinus* and strain CM12 were calculated [35] and they were found to be 79% and 65%, respectively. Thus, more than half of the cellulose isolated from *Synechococcus* 7002 strain CM12 was in crystalline and/or microcrystalline form, but it contained less type-I cellulose than the cellulose fibers isolated from *G. xylinus*.

Discussion

In this study we show that the *cesA* (SYNPCC7002_A2118) gene product is required for the production of a distinctive cell wall layer in *Synechococcus* 7002. This layer is most likely localized between the PG layer and the outer membrane and is possibly laminated. CesA also contributed to the production of polysaccharides associated with the glycocalyx. Three lines of evidence indicate that this polysaccharide is cellulose. First, *Synechococcus* 7002 CesA is required for the production of this polysaccharide, and this protein has strong sequence similarity to bacterial cellulose synthases as well as to CesA from *Nostoc* sp. PCC 7120, a cyanobacterium that has previously been shown to synthesize cellulose [23]. Second, in the presence of EDTA, some (but not all) of the extracellular glycocalyx as well as the

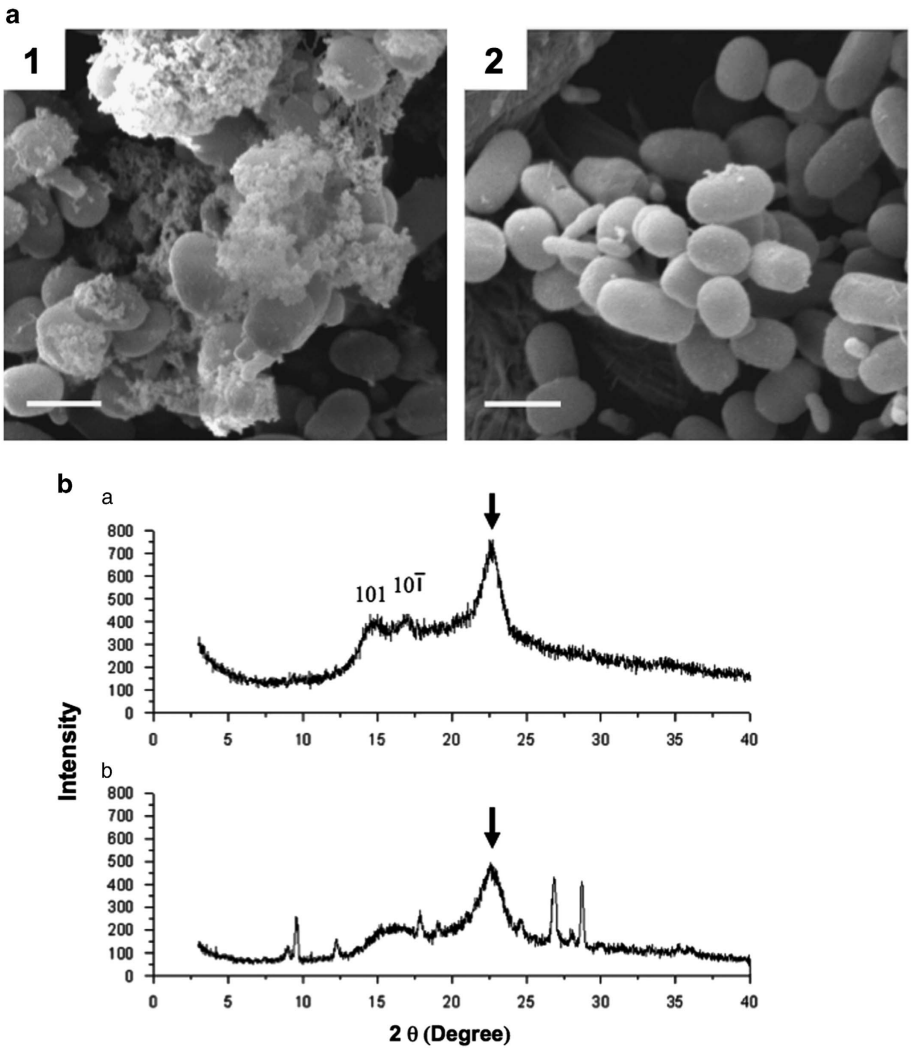

Figure 7 Analysis of cellulose fibers produced by strain CM12 of *Synechococcus* 7002. (**a**) Scanning electron microscopy (SEM) analysis of extracellular cellulose fibers. Strain CM12 cells were grown in medium BG-11 for 12 days and were prepared for SEM examination without (1) or with cellulase treatment (2) for 30 min. Scale bar, 2 μm. (**b**) X-ray diffraction analysis of the cellulose isolated from *G. xylinus* (a) and from *Synechococcus* 7002 strain CM12 (b). Arrows indicate the position of peak 002.

periplasmic layer could be digested with cellulase, which indicates that the polysaccharides found in the digestible fraction contain β-1,4-glucosidic bonds. Third, the polysaccharide in the periplasmic space and the glycocalyx could be specifically labeled with a recombinant cellulose-binding domain (Figure 3) and was missing in a *cesA* mutant. Collectively, these data establish that the cell walls and glycocalyx of *Synechococcus* 7002 contain cellulose that is produced by the action of CesA.

To obtain very high levels of cellulose production in *Synechococcus* 7002, it was necessary to introduce six genes, *cmc–ccp–cesAB–cesC–cesD–bgl,* from *G. xylinus* into this cyanobacterium. Polymerization and crystallization are coupled in cellulose synthesis in *G. xylinus* and are thought to be the rate-liming steps in these processes [9, 36]. Because the strains with only the *cesAB–cesC–cesD* operon did not produce detectable extracellular cellulose, the high-yield production of extracellular crystalline cellulose in strain CM12 strongly suggested that the genes flanking the *cesAB–cesC–cesD* operon are essential for cellulose synthesis in *Synechococcus* 7002. Previous studies have shown that the products of the *cmc* (endo-β-1,4-glucanase) and *ccp* genes upstream of *cesA* and the downstream *cesD* and *bgl* genes are involved in cellulose production and/or crystallization [11, 12, 14, 20, 21, 37, 38]. When only the *cesAB* genes were introduced into a

cyanobacterium, only amorphous cellulose was produced [39]. These observations further support the idea that genes other than those encoding the cellulose synthase (that is, other than *cesAB*/*bcsAB*) [18] are important for high-yield production of cellulose in bacteria. Therefore, the cluster of six genes (*cmc–ccp–cesAB–cesC–cesD–bgl*) from *G. xylinus* can be regarded as a complete CSM module for bacterial cellulose synthesis, even though we cannot completely rule out the possibility that some factors could be provided by *Synechococcus* 7002 for this process. For example, it is known that cyclic-di-GMP is required for bacterial cellulose synthesis [8]. The *Synechococcus* 7002 genome predicts three diguanylate cyclases and one enzyme for degradation of cyclic-di-GMP, and it is therefore highly likely that this cyanobacterium can produce the cyclic-di-GMP required to activate the cellulose synthase of *G. xylinus*. As noted above, it is possible that low-salinity growth conditions might activate the production of cylic-di-GMP in *Synechococcus* 7002, which could in turn activate the cellulose synthase via its PilZ domain.

The high-yield production of cellulose by cyanobacteria using only light and inorganic nutrients has potential uses for bioenergy as well as traditional industries that use cellulose. Assuming that cellulose produced by *Synechococcus* 7002 could be converted to ethanol at 70% efficiency, this system could yield ~4 500 gallons of ethanol per acre-ft per year if the biomass were harvested every 3 weeks at a final dry weight concentration of 20 mg/l. Even if cellulose production were only feasible for 6 months per year, *Synechococcus* 7002 would still yield sixfold more ethanol than corn, which typically yields 300–400 gallons of ethanol per acre per year [40]. A potentially interesting application of the findings reported here would be to couple cellulose production by *Synechococcus* 7002 to triglyceride synthesis in a cellulose-degrading, biodiesel-producing, eukaryotic alga such as *Chlamydomonas reinhardtii* [41]. Alternatively, large-scale cellulose synthesis could facilitate CO_2 sequestration. Marine cyanobacteria and algae are widely believed to have important roles in the carbon cycle by removing of CO_2 from the atmosphere [42, 43]. Because cellulose degradation occurs more slowly in the open ocean than in coastal and terrestrial areas [44], cellulose production and/or deposition in the open ocean could lead to carbon sequestration. Extracellular cellulose might promote fixed-carbon deposition by enhancing the formation of larger, more rapidly sedimenting cell aggregates. Finally, bacterial cellulose has shown significant potential for biomedical applications, especially for wound care and the regeneration of damaged organs [5].

Materials and Methods

Strains and culture conditions

Synechococcus sp. strain PCC 7002 WT, *cesA* mutant strains, and engineered strains were grown in a high-salinity (marine) A^+ medium or low-salinity BG-11 medium (BG-11 used in this work was always added with vitamin B_{12} at a final concentration of 4 μg/l) [45, 46] with appropriate antibiotics when needed at 35 °C under cool-white fluorescent light at ~150 μmol/m^2/s. The cultures were sparged with air plus 1% (v/v) CO_2. *Gluconacetobacter xylinus* ATCC 53582 was cultured according to instructions provided by American Type Culture Collections (www.atcc.org). *Escherichia coli* strain DH5α was used for all routine recombinant DNA procedures.

Construction of cesA insertion and deletion mutant strains

Insertional inactivation (Supplementary Figure S5) of *the cesA* gene (SYNPCC7002_A2118) of *Synechococccus sp.* PCC 7002 (*Synechococcus* 7002) was performed as follows: a 4.37-kb DNA fragment containing *cesA* plus flanking 1-kb upstream and 1-kb downstream regions was amplified by PCR using total chromosomal DNA as template with *TransStart FastPfu* DNA polymerase (Transgen, Beijing, China).

The primers used for the PCR were 5′-CGATATTCACA CGGCTATTGGCCCG-3′ and 5′-CCAGGGAAATTGCAA CAGACGGAGC-3′. The amplified fragment was cloned into the *pEASY*-Blunt Simple Cloning Vector (Transgen). The resultant plasmid was then used as the PCR template with the primers 5′-CAATTGCTGTGTATACTTATCAACTTCGGC TTCT-3′ and 5′-ATCGATCTCCCCAGATGTCGCTACAT TGCT-3′ to generate a blunt-ended DNA fragment, which was ligated to a 1.3-kb blunt-ended DNA fragment encoding the *aphA-II* gene (conferring resistance to kanamycin) and transformed into *E. coli*. The plasmid was then isolated and transformed into *Synechococcus* 7002 for construction of a *cesA* mutant.

Complete deletion of *cesA* in PCC 7002 was performed as previously described [47]. Flanking regions of *cesA* were amplified from *Synechococcus sp* PCC 7002 genomic DNA using the following primers: upstream region: 5′-TAGTCTGT AAACCTTCCGATGCATCTTCAGAGGATGTAGATGT-3′ and 5′-CGCATTAATAATGTATGCTAGCGGAGTGTGAC TCGTTTGT-3′ and downstream region: 5′-TCAAATATTTT TCTTTTTGGTACCAATAATGGCCTTGATCTGG-3′ and 5′-GCAATCACCAATAACAAAGCATGCTCAAGAAGAC AAACATAC-3′. Restriction sites are underlined. The two PCR products were digested with *Nsi*I, *Nhe*I and *Kpn*I, and *Sph*I, respectively. A chloramphenicol resistance cassette was excised from pRL409 [48] with *Nhe*I and *Kpn*I. The plasmid pGEM-7zf was digested with *Nsi*I and *Sph*I. The PCR products, antibiotic resistance cassette, and the pGEM-7zf were ligated to form a new plasmid in which the upstream and downstream flanking regions of *cesA* flanked the *cat* gene. This plasmid was digested with *Nsi*I and used to transform *Synechococcus* 7002. Transformants carrying the *cesA* deletion mutation were

selected on A^+ medium supplemented with chloramphenicol (10 μg/ml). Complete segregation of the WT and *cesA* deletion alleles was verified by PCR analysis using primers *cesA*-For 5′-CTATGAAGGCCATACAAGAGAAATGCG-3′ and *cesA*-Rev 5′-TCAAGAATCACAAATTCCTTAGACATG AGC-3′.

Construction of cesA::yfp fusion gene

Overexpression of a CesA–YFP fusion protein in a *cesA* deletion mutant of *Synechococcus* 7002 was performed according to Xu *et al.* [28]. Full-length *cesA* was amplified from genomic DNA of *Synechococcus* 7002 with Platinum Pfx DNA polymerase (Invitrogen, Grand Island, NY, USA) using the following primers: forward: 5′-TATTCATTTTATTTATCA CATATGTTGGAACTAGTCCCTTCATTTAAAAACAAA CGAGTC-3′ and reverse: 5′-TTACTTGTCTCCTAAAAC CATATGTTGTTCTTCTGGCTGCCAGTAAG-3′. The TAA stop codon of the *cesA* gene was changed to CAT in the reverse primer. The full-length *cesA* gene in this PCR product started and ended with 5′-CATATG-3′ (*Nde*I sites). After digestion with *Nde*I, the PCR product was inserted into the *Nde*I site of the plasmid pAQ1-EX-P_{cpcBA}::*yfp*, to produce pAQ1-EX-P_{cpcBA}::*cesA-yfp* (Supplementary Figure S6). Plasmids with the *cesA* insert were sequenced to determine the orientation of the *cesA* insertion and to verify the *cesA* sequence. One plasmid with correct orientation and sequence was used to transform the *cesA* deletion mutant of *Synechococcus* 7002. Selection for the complemented transformants was performed on medium A^+ supplemented with 10 μg/ml chloramphenicol and 100 μg/ml spectinomycin. Transcription of *cesA::yfp* in complemented mutant was confirmed by reverse transcriptase-PCR.

Immunogold labeling

Immunogold labeling of thin sections was performed by a procedure similar to that described by Nobles *et al.* [23]. Cells were fixed 2% (w/v) paraformaldehyde and 0.5% (v/v) glutaraldehyde in 0.1 M phosphate buffer (PB), pH 7.2, for 30 min and transferred to fresh fixative for another 3 h at room temperature. After washing three times with 0.1 M PB, cells were embedded in 0.5 ml of 3% (w/v) agarose dissolved in 0.1 M PB buffer at 40 °C. After cooling and solidification, the agarose was cut into ~1-mm^3 blocks, which were washed and dehydrated in 50, 70, 90, and 100% (v/v) ethanol. The blocks were embedded in London Resin White and polymerized at 60 °C for 24 h. After ultrathin sectioning, the grids were washed with phosphate-buffered saline (PBS), pH 7.4, for 1 min and then incubated in 1:20 000 dilution of rCBD-Protein-L (Fluka Sigma-Aldrich, Buchs, Switzerland) in PBS at room temperature for 1 h. The grids were washed five times with PBS for 5 min and were blocked in 0.5% bovine serum albumin in PBS for 30 min. The grids were incubated in 1:50 goat anti-mouse IgG 10-nm gold conjugate (British Biocell International, Cardiff, UK) for 1 h at room temperature and were stained with 1% (w/v) glutaraldehyde for 5 min followed by washing with PBS three times and with water five times. The grids were stained with 1% (w/v) uranyl acetate for 5 min and washed with water five times. Grids were dried in air, and samples were observed with a JEM-1200EX electron microscope (JEM, Tokyo, Japan).

Construction of the BAC Library of G. xylinus

Construction of the *G. xylinus* BAC library was performed using the Epicentre CopyControl BAC Cloning Kit protocol (Epicentre, Madison, WI, USA, Cat. No. CCBAC1B), except that a 1.2-kb DNA fragment from *Synechococcus* 7002 and an erythromycin resistance cartridge was inserted to the *Sca*I site of the pCC1BAC Vector (Epicentre) so the resulting BAC plasmids could be integrated into the *Synechococcus* 7002 genome through a single recombinant event. The 1.2-kb DNA fragment from *Synechococcus* 7002 genome was amplified by PCR with primers 5′-CACGGTAGAATCCTCCGCCTGGGCC-3′ and 5′-TTGACTGCACCAATGGAGAAAC-3′. For cloning of a fragment encoding the six genes responsible for cellulose synthesis and extrusion from *G. xylinus* (*cmc–ccp–cesAB–cesC–cesD–bgl*, CSM), PCR was performed with the following primers: 5′-GAGATCTAGACGTTCCTTTATGTCGGTCATG GC-3′ and 5′-TATAGGATCCCCATACTCAGGGGGCCA TGTT-3′. The fragment was then integrated into the pQ1 vector with the erythromycin resistance cartridge according to Xu *et al.* [28]. The genes were under the control of the promoter P_{cpcBA} from *Synechocystis sp*. PCC 6803 [28].

Fluorescence and electron microscopy

Fluorescence microscopy was performed with an Olympus BX51 microscope (Olympus, Tokyo, Japan) and a Zeiss LSM 510 Live Confocal Microscope (Zeiss, Peabody, MA, USA). Low-temperature (77 K) fluorescence emission spectra were measured for cells grown at different light conditions using an SLM8000-based spectrofluorometer modified for computerized, solid-state operation by On-Line Instrument Systems Inc. (Bogart, GA, USA) as described previously [49]. Transmission electron microscopy of thin sections was performed with a JEM-1010 electron microscope (Jeol, Tokyo, Japan). Sample preparation and thin sectioning were carried out as described [50]. Scanning electron microscopy images were obtained using a field emission scanning electron microscope (FEI Quanta 200 F, Eindhoven, The Netherlands), and sample preparation was based on the protocol described [51].

Cell wall preparation and quantitative determination of cellulose

Cyanobacterial cell wall specimens were prepared as described [52] and quantitation of total glucose was performed using the anthrone–sulfuric acid method [53].

X-ray diffraction

The X-ray diffraction profiles of cellulose specimens were obtained by DMAX-2400 (Rigaku, Japan) with Cu Kα radiation. The X-ray diffraction pattern was collected at a continuous scan mode with step of 0.02° at the rate of 2°/min in the 2θ-range of 0–50°.

Acknowledgements

This work was supported by grants from the Ministry of Science and Technology of China (2009AA021405 and 2015CD150101) and the CAS International Partnership Program for Research Teams to JZ. Work in the laboratory of

DAB was supported by Air Force Office of Scientific Research MURI grant FA9550-05-1-0365. We thank Nicole Zembower and Susan Magargee for assistance with confocal imaging, and Dr. Gang Ning and Missy Hazen at the Microscopy and Cytometry Facility of the Huck Institutes of the Life Sciences (Penn State University, University Park), Yingchun Hu at College of Life Sciences, Peking University and Jingnan Liang at Institute of Microbiology, Chinese Academy of Sciences for the help with transmission electron microscopy, Chunli Li at Institute of Microbiology, Chinese Academy of Sciences for the help with scanning electron microscopy, and Fuhui Liao at College of Chemistry & Molecular Engineering, Peking University for help with X-ray diffraction.

References

1 Tilman D, Hill J, Lehman C. Carbon-negative biofuels from low-input high-diversity grassland biomass. *Science* 2006; **314**: 1598–1600.
2 Goldemberg J. Ethanol for a sustainable energy future. *Science* 2007; **315**: 808–810.
3 Yuan JS, Tiller KH, Al-Ahmad H, Stewart NR, Stewart CN Jr. Plants to power: bioenergy to fuel the future. *Trends Plant Sci* 2008; **13**: 421–429.
4 Carroll A, Somerville C. Cellulosic biofuels. *Annu Rev Plant Biol* 2009; **60**: 165–182.
5 Czaja WK, Young DJ, Kawecki M, Brown RM Jr. The future prospects of microbial cellulose in biomedical applications. *Biomacromolecules* 2007; **8**: 1–12.
6 Ross P, Mayer R, Benziman M. Cellulose biosynthesis and function in bacteria. *Microbiol Rev* 1991; **55**: 35–58.
7 Somerville C. Cellulose synthesis in higher plants. *Annu Rev Cell Dev Biol* 2006; **22**: 53–78.
8 Delmer DP. Cellulose biosynthesis: exciting times for a difficult field of study. *Annu Rev Plant Physiol Plant Mol Biol* 1999; **50**: 245–276.
9 Saxena IM, Brown RM Jr. Cellulose biosynthesis: current views and evolving concepts. *Ann Bot* 2005; **96**: 9–21.
10 Mutwil M, Debolt S, Persson S. Cellulose synthesis: a complex complex. *Curr Opin Plant Biol* 2008; **11**: 252–257.
11 Hu SQ, Gao YG, Tajima K, *et al.* Structure of bacterial cellulose synthase subunit D octamer with four inner passageways. *Proc Natl Acad Sci USA* 2010; **107**: 17957–17961.
12 Sunagawa N, Fujiwara T, Yoda T, *et al.* Cellulose complementing factor (Ccp) is a new member of the cellulose synthase complex (terminal complex) in *Acetobacter xylinum*. *J Biosci Bioeng* 2013; **115**: 607–612.
13 Wong HC, Fear AL, Calhoon RD, *et al.* Genetic organization of the cellulose synthase operon in *Acetobacter xylinum*. *Proc Natl Acad Sci USA* 1990; **87**: 8130–8134.
14 Saxena IM, Kudlicka K, Okuda K, Brown RM Jr. Characterization of genes in the cellulose-synthesizing operon (*acs* operon) of *Acetobacter xylinum*: implications for cellulose crystallization. *J Bacteriol* 1994; **176**: 5735–5752.
15 Kawano S, Tajima K, Uemori Y, *et al.* Cloning of cellulose synthesis related genes from *Acetobacter xylinum* ATCC23769 and ATCC53582: comparison of cellulose synthetic ability between strains. *DNA Res* 2002; **9**: 149–156.
16 Brown RM Jr, Willison JH, Richardson CL. Cellulose biosynthesis in *Acetobacter xylinum*: visualization of the site of synthesis and direct measurement of the *in vivo* process. *Proc Natl Acad Sci USA* 1976; **73**: 4565–4569.
17 Kimura S, Chen HP, Saxena IM, Brown RM Jr, Itoh T. Localization of c-di-GMP-binding protein with the linear terminal complexes of *Acetobacter xylinum*. *J Bacteriol* 2001; **183**: 5668–5674.
18 Morgan JL, Strumillo J, Zimmer J. Crystallographic snapshot of cellulose synthesis and membrane translocation. *Nature* 2013; **493**: 181–186.
19 Whitney JC, Hay ID, Li C, *et al.* Structural basis for alginate secretion across the bacterial outer membrane. *Proc Natl Acad Sci USA* 2011; **108**: 13083–13088.
20 Tonouchi N, Tahara N, Kojima Y, *et al.* A beta-glucosidase gene downstream of the cellulose synthase operon in cellulose-producing *Acetobacter*. *Biosci Biotechnol Biochem* 1997; **61**: 1789–1790.
21 Saxena IM, Lin FC, Brown RM Jr. Identification of a new gene in an operon for cellulose biosynthesis in *Acetobacter xylinum*. *Plant Mol Biol* 1991; **16**: 947–954.
22 Richmond T. Higher plant cellulose synthases. *Genome Biol* 2000; **1**: REVIEWS3001.1–3001.6.
23 Nobles DR, Romanovicz DK, Brown RM Jr. Cellulose in cyanobacteria. Origin of vascular plant cellulose synthase?. *Plant Physiol* 2001; **127**: 529–542.
24 Kawano Y, Saotome T, Ochiai Y, Katayama M, Narikawa R, Ikeuchi M. Cellulose accumulation and a cellulose synthase gene are responsible for cell aggregation in the cyanobacterium *Thermosynechococcus vulcanus* RKN. *Plant Cell Physiol* 2011; **52**: 957–966.
25 Ludwig M, Bryant DA. *Synechococcus* sp. strain PCC 7002 transcriptome: acclimation to temperature, salinity, oxidative stress, and mixotrophic growth conditions. *Front Microbio* 2012; **3**: 354.
26 Hoiczyk E, Hansel A. Cyanobacterial cell walls: news from an unusual prokaryotic envelope. *J Bacteriol* 2000; **182**: 1191–1199.
27 Fletcher M, Floodgate GD. An electron-microscopic demonstration of an acidic polysaccharide involved in the adhesion of a marine bacterium to solid surfaces. *J Gen Microbiol* 1973; **74**: 325–334.
28 Xu Y, Alvey RM, Byrne PO, Graham JE, Shen G, Bryant DA. Expression of genes in cyanobacteria: adaptation of endogenous plasmids as platforms for high-level gene expression in *Synechococcus* sp. PCC 7002. *Methods Mol Biol* 2011; **684**: 273–293.
29 Herth W, Schnepf E. The fluorochrome, calcofluor white, binds oriented to structural polysaccharide fibrils. *Protoplasma* 1980; **105**: 129–133.
30 Xu Y, Guerra LT, Li Z, Ludwig M, Dismukes GC, Bryant DA. Altered carbohydrate metabolism in glycogen synthase mutants of *Synechococcus* sp. strain PCC 7002: cell factories for soluble sugars. *Metab Engin* 2013; **16**: 56–67.

31 Guerra LT, Xu Y, Bennette N, McNeely K, Bryant DA, Dismukes GC. Natural osmolytes are much less effective substrates than glycogen for catabolic energy production in the marine cyanobacterium *Synechococcus* sp. strain PCC 7002. *J Biotechnol* 2013; **166**: 65–75.
32 Fujiwara T, Komoda K, Sakurai N, Tajima K, Tanaka I, Yao M. The *c*-di-GMP recognition mechanism of the PilZ domain of bacterial cellulose synthase subunit A. *Biochem Biophys Res Commun* 2013; **431**: 802–807.
33 Atalla RH, Vanderhart DL. Native cellulose: a composite of two distinct crystalline forms. *Science* 1984; **223**: 283–285.
34 Haigler CH, Brown RM Jr, Benziman M. Calcofluor white ST alters the *in vivo* assembly of cellulose microfibrils. *Science* 1980; **210**: 903–906.
35 Segal L, Creely JJ, Martin AE Jr, Conrad CM. An empirical method for estimating the degree of crystallinity of native cellulose using the X-ray diffractometer. *Tex Res J* 1962; **29**: 786–794.
36 Benziman M, Haigler CH, Brown RM Jr, White AR, Cooper KM. Cellulose biogenesis: polymerization and crystallization are coupled processes in *Acetobacter xylinum*. *Proc Natl Acad Sci USA* 1980; **77**: 6678–6682.
37 Koo HM, Song SH, Pyun YR, Kim YS. Evidence that a beta-1,4-endoglucanase secreted by *Acetobacter xylinum* plays an essential role for the formation of cellulose fiber. *Biosci Biotechnol Biochem* 1998; **62**: 2257–2259.
38 Nakai T, Nishiyama Y, Kuga S, Sugano Y, Shoda M. ORF2 gene involves in the construction of high-order structure of bacterial cellulose. *Biochem Biophys Res Commun* 2002; **295**: 458–462.
39 Nobles DR, Brown RM Jr. Transgenic expression of *Gluconacetobacter xylinus* strain ATCC 53582 cellulose synthase genes in the cyanobacterium *Synechococcus leopoliensis* strain UTCC 100. *Cellulose* 2008; **15**: 691–701.
40 Wallington TJ, Anderson JE, Mueller SA, *et al.* Corn ethanol production, food exports, and indirect land use change. *Environ Sci Technol* 2012; **46**: 6379–6384.
41 Blifernez-Klassen O, Klassen V, Doebbe A, *et al.* Cellulose degradation and assimilation by the unicellular phototrophic eukaryote *Chlamydomonas reinhardtii*. *Nat Commun* 2012; **3**: 1214.
42 Field CB, Behrenfeld MJ, Randerson JT, Falkowski P. Primary production of the biosphere: integrating terrestrial and oceanic components. *Science* 1998; **281**: 237–240.
43 Falkowski PG. The ocean's invisible forest. *Sci Am* 2002; **287**: 54–61.
44 Strand SE, Benford G. Ocean sequestration of crop residue carbon: recycling fossil fuel carbon back to deep sediments. *Environ Sci Technol* 2009; **43**: 1000–1007.
45 Stevens SE Jr, Patterson COP, Myers J. The production of hydrogen peroxide by blue-green algae: A survey. *J Phycol* 1973; **9**: 427–430.
46 Rippka R, Deruelles J, Waterbury JB, Herdman M, Stanier RY. Generic assignments, strain histories and properties of pure cultures of cyanobacteria. *J Gen Microbiol* 1979; **111**: 1–61.
47 Frigaard NU, Sakuragi Y, Bryant DA. Gene inactivation in the cyanobacterium *Synechococcus* sp. PCC 7002 and the green sulfur bacterium *Chlorobium tepidum* using in vitro-made DNA constructs and natural transformation. *Methods Mol Biol* 2004; **274**: 325–340.
48 Elhai J, Wolk CP. A versatile class of positive-selection vectors based on the nonviability of palindrome-containing plasmids that allows cloning into long polylinkers. *Gene* 1988; **68**: 119–138.
49 Shen G, Bryant DA. Characterization of a *Synechococcus* sp. Strain PCC 7002 mutant lacking photosystem I. Protein assembly and energy distribution in the absence of the photosystem I reaction center core complex. *Photosynth Res* 1995; **44**: 41–53.
50 Ohki K, Fujita Y. Photoregulation of phycobilisome structure during complementary chromatic adaptation in the marine cyanophyte *Phormidium* sp. C86. *J Phycol* 1992; **28**: 803–808.
51 Albertano P, Urzi C. Structural interactions among epilithic cyanobacteria and heterotrophic microorganisms in Roman hypogea. *Microbial Ecol* 1999; **38**: 244–252.
52 York WS, Darvill AG, McNeil M, Stevenson TT, Albersheim P. Isolation and characterization of plant cell walls and cell wall components. *Methods Enzymol* 1986; **118**: 3–40.
53 Updegraff DM. Semimicro determination of cellulose in biological materials. *Anal Biochem* 1969; **32**: 420–424.

(**Supplementary Information** is linked to the online version of the paper on the *Cell Discovery* website.)